

## Design of Dielectric Resonator Antenna by (1-x) MZTO-(x) CSTO Microwave Dielectric Ceramic\*

**Shailendra Singh Rajput and Sunita Keshri**

Department of Applied Physics  
Birla Institute of Technology, Mesra, Ranchi-835215, India  
Email: s\_keshri@bitmesra.ac.in

(Received June 14, 2011)

**Abstract:** In this paper we present the studies on microwave dielectric composites,  $(1-x)(\text{Mg}_{0.95}\text{Zn}_{0.05})\text{TiO}_3-x(\text{Ca}_{0.8}\text{Sr}_{0.2})\text{TiO}_3$ . The materials have been prepared by solid state method and the co-existence of both the phases with no traceable interdiffusion has been confirmed by the studies done using X-ray Diffractometer and Scanning Electron Microscope. The microwave dielectric properties of these composite materials have also been investigated. We have observed a dielectric constant ( $\epsilon_r$ ) of 21.9, a dielectric loss  $[(\tan \delta)]$  of 0.0002, and temperature coefficient of resonant frequency ( $\tau_f$ ) of  $-0.15 \text{ ppm/}^\circ\text{C}$  for  $0.92(\text{Mg}_{0.95}\text{Zn}_{0.05})\text{TiO}_3-0.08(\text{Ca}_{0.8}\text{Sr}_{0.2})\text{TiO}_3$  ceramic, sintered at  $1300^\circ\text{C}$  for 4 h which is found suitable for antenna application. We have designed the cylindrical dielectric resonator antenna (DRA) using this material; the DRA has been excited by coaxial probe feeding mechanism. The variations of return loss versus frequency and far field radiation patterns of the DRA at the respective resonant frequency have been simulated by finite element method (Ansoft High Frequency Structure Simulator). The simulated results have been compared with the measured results and a good agreement is achieved between these results.

**Keyword:** Dielectric composite; Dielectric Resonator; Return loss; Bandwidth; Radiation pattern.

### 1. Introduction

Dielectric resonators (DRs) are extensively used in microwave components such as filters, duplexers, oscillators and patch antennas for cellular phones and global positioning systems. When a dielectric resonator is not entirely enclosed by a conducting boundary, it can radiate, and so it becomes an antenna, named dielectric resonator antenna (DRA). Currently DRA is one of the popular choices for MW, millimeter wave band and above<sup>1, 2</sup>. The use of DRA has been widely accepted since the original paper on the cylindrical DRA<sup>3</sup>. DRAs have useful properties such as broad

---

\*Paper presented in CONIAPS XIII at UPES, Dehradun during June 14-16, 2011.

bandwidth, low profile, resistance to proximity detuning, and high radiation efficiency flexible feed arrangement, simple geometry, and compactness<sup>4-8</sup>. Kingsley and O'Keefe<sup>9, 10</sup> manipulated the radiation pattern of dielectric resonator antennas in the azimuth plane by exciting different probes within the same dielectric. As compared to microstrip antenna, DRAs have much wider impedance bandwidth and they don't support surface waves and microstrip antennas have limitations in their size, bandwidth, and efficiency. The resonance mode used for radiation depends on the geometry of the resonator and the required radiation pattern. The fields of the mode should not be strongly confined within the resonator and therefore, it can be easily fed to produce high efficiency radiation<sup>8</sup>. For DRA applications, the dielectric materials must possess the combined dielectric properties of a high dielectric constant( $\epsilon_r$ ), a low dielectric loss (high  $Q \times f$  value) and a near zero temperature coefficient of resonant frequency ( $\tau_f$ ) as small as possible. These three parameters are correlated to the size, the frequency selectivity and the temperature stability of the devices, respectively<sup>11</sup>. One thing is very important that in microwave circuits, each dielectric property controlled very precisely. It is found that by using two or more compounds with negative and positive temperature coefficients is the most promising method of obtaining a zero temperature coefficient of resonant frequency<sup>12</sup>.

In the recent years magnesium titanate ( $\text{MgTiO}_3$ ) is one of the leading dielectric materials for microwave frequency applications as dielectrics in resonators, filters and antennas for communication, radar, and global positioning systems (GPS) operating at microwave frequencies<sup>12, 13</sup>.  $\text{MgTiO}_3$ - $\text{CaTiO}_3$  (MCT) with the partial replacement of Mg and Ca is well known as a material used in temperature-compensating capacitors, dielectric resonators, and patch antennas<sup>14, 15</sup>. The  $(\text{Mg}_{0.95}\text{Zn}_{0.05})\text{TiO}_3$  (MZTO) ceramic was investigated to possess excellent dielectric properties with an  $(\epsilon_r) \sim 16.21$ ,  $Q \times f$  value  $\sim 240,000$  (GHz) and a large negative  $(\tau_f) \sim -60$  ppm/ $^\circ\text{C}$ <sup>16, 17</sup>. Instead of  $(\text{Ca}_{0.8}\text{Sr}_{0.2})\text{TiO}_3$  (CSTO) ceramic, having dielectric properties of  $(\epsilon_r) \sim 181$ ,  $Q \times f$  value  $\sim 8,300$  (GHz) and a large positive  $(\tau_f) \sim 991$  ppm/ $^\circ\text{C}$ <sup>18</sup>, was chosen as a  $\tau_f$  compensator for  $(\text{Mg}_{0.95}\text{Zn}_{0.05})\text{TiO}_3$ .

In this study, the microwave dielectric properties, including a high dielectric constant, a low dielectric loss and a nearly zero  $\tau_f$  value, have

been considered in order to realize an outstanding design of the DRA having a small size and high temperature stability with high radiation efficiency. The coaxial probe feed mechanism are used for excitations. The variations of return loss vs. frequency and far field radiation patterns of the DRAs are determined experimentally at their respective resonant frequencies in C-band of Radar frequency range. The measured results for both DRAs are compared with those simulated results and an excellent agreement has been achieved.

## 2. Experimental

The dielectric composites  $(1-x)\text{MZTO} - (x)\text{CSTO}$  where  $x = 0.2, 0.3, 0.4, 0.5, 0.6$  and  $0.8$  (here after referred as 98MZCST, 97MZCST, 96MZCST, 95MZCST, 94MZCST, and 92MZCST respectively) were prepared using the conventional solid state mixed ceramic route in two steps. In the first step MZTO and CSTO were synthesized from the raw materials  $\text{MgO}$ ,  $\text{TiO}_2$ ,  $\text{ZnO}$ ,  $\text{CaCO}_3$ ,  $\text{SrCO}_3$  powders. The stoichiometric amount of raw materials were accurately weighed and mixed with distilled water for 24 h in a ball mill using zirconia balls. The dried powders were calcined at  $1100^\circ\text{C}$  for 4 hrs<sup>17, 18</sup>. In the second step the calcined reagents were mixed as desired composition and remilled for 24 h. PVA solution of 3wt% was added to the samples and pressed in the form of cylindrical disc of diameter 8mm and height 5mm. These pellets were sintered at  $1300^\circ\text{C}$  for 4 hrs in air. Crystallographic structure of the specimen was examined at room temperature by the X-ray diffraction (XRD; Philips,  $\text{CuK}_\alpha$  radiation) with a step size of 0.02 in the range of  $10^\circ \leq 2\theta \leq 80^\circ$ . The surface morphology of the samples was studied using JEOL scanning electron microscope (SEM; JEOL, Model: JSM-6390LV) equipped with Energy dispersive X-ray (EDX) Spectrometer (Oxford INCA, Model: DCL-7673). Calculation of the dielectric permittivity and losses from the measured resonance frequency and Q-factor was performed by the program (provided by J. Krupka) which is based on the electro dynamical analysis and accounts parameters of our cavity. The temperature coefficients of the resonant frequency ( $\tau_f$ ) were defined as follows:

$$\tau_f = \frac{f_2 - f_1}{f_1(T_2 - T_1)}$$

where  $f_1$  and  $f_2$  represent the resonant frequencies at  $T_1$  and  $T_2$ , respectively. The cylindrical DRA is worked at the  $HEM_{116}$  mode, whose resonant frequency  $f_0$  can be approximated<sup>19</sup> by

$$f_0 = \frac{2.997}{20\pi\sqrt{2+\epsilon_r}} \left[ 0.27 + 0.36 \frac{a}{2h} + 0.02 \left( \frac{a}{2h} \right)^2 \right],$$

where  $\epsilon_r$  is the dielectric constant,  $a$  and  $h$  are the radius and thickness of DRA. The characteristic of this antenna have been simulated by using the Ansoft High Frequency Structure Simulator (HFSS) based upon the Finite Element Method.

### 3. Results and Discussion

#### 3.1. Structural and dielectric properties

X-ray diffraction (XRD) patterns of MZTO, CSTO and 92MZCST ceramics are shown in Fig. 1. It is observed from the figure that MZTO presents as the main crystalline phase, in association with minor phase

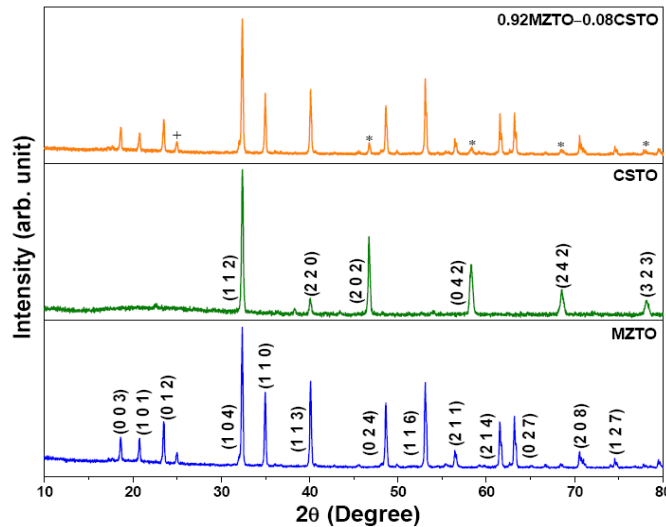
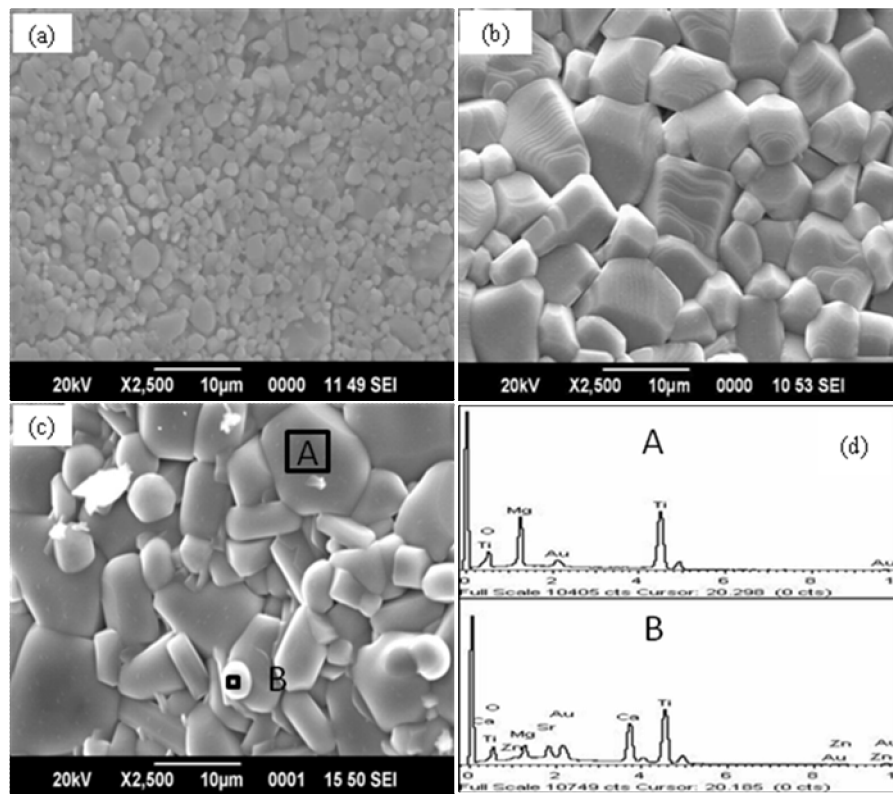


Figure1. XRD patterns of MZTO, CSTO and 92MZCST samples

CSTO. An intermediate phase  $(Mg_{0.92}Zn_{0.08})Ti_2O_5$  is usually formed (ICDD–PDF #00–009–0016) and is difficult to completely eliminate from the samples prepared using the mixed oxide. With increasing CSTO content, intensity corresponding to pure MZTO phase decreases and that of CSTO increases. By employing ‘Checkcell’ software it is observed that MZTO has a rhombohedral structure with lattice constants  $a = 5.152(1)$  Å,  $b =$

5.152(2) Å, and  $c = 13.856(1)$  Å having  $R\bar{3}C$  space group whereas pure CSTO has an orthorhombic structure with lattice constants  $a = 5.469(1)$  Å,  $b = 5.457(1)$  Å, and  $c = 7.706(2)$  Å having  $Pbnm$  space group. The SEM images of the CSTO, MZTO and 92MZCST samples are shown in Fig. 2. From figures it can be observed that in composite sample grains of both the phases are clearly distinguishable from each other. CSTO grains are distributed randomly beside MZTO grains, grains corresponding to both the phases have been identified by EDX analysis. EDX analysis was used in combination with scanning electron microscopy to distinguish each grain of 92MZCST ceramics. The peaks in the EDX spectra come from the coating of gold over the surface of sample required to avoid charging. The grain size decreased with the increase of x values due to more existing CSTO phase.



**Fig. 2.** SEM micrographs of (a) CSTO, (b) MZTO, (c) 92MZCST; (d) shows the EDX results of the regions "A" and "B" taken across the grain boundary of 92MZCST sample.

The dielectric constant and loss tangent of (1-x)MZTO– (x)CSTO ceramic system with variation of CSTO percentage in the microwave frequency range are enlisted in Table 1. The dielectric constant increases from 18.6 to 21.9 and the loss tangent also increases from 0.00009 to 0.0002 with increasing CSTO addition because the CSTO having high dielectric constant and high loss compared to MZTO. Many factors are believed to simultaneously affect the dielectric loss. The formation of a second phase ( $\text{Mg}_{0.95}\text{Zn}_{0.05}\text{Ti}_2\text{O}_5$ ) during sample preparation is also a reason of higher loss. The temperature coefficient of resonant frequency ( $\tau_f$ ) values for all the samples are enlisted in Table 1. It is observed that the  $\tau_f$  values of samples rapidly increased with increasing CSTO content due to a large positive  $\tau_f$  of CSTO ( $\tau_f \sim 991$  ppm/°C). It varied from –49.96 to –0.15 ppm/°C as the amount of CSTO addition increases from 0.02 to 0.08. Hence a nearly zero  $\tau_f$  value is achieved for the 92MZCST sample, which is proposed for designing the DRA.

Table1. Microwave dielectric properties of MZTO–CSTO system

% CSTO	$\epsilon_r$	$\tan \delta$	$Q \times f$ (GHz)	$\tau_f$ (ppm/°C)
2	18.6	9E–5	94711.76	–49.96
3	19.65	1.14E–4	79487.63	–41.54
4	19.9	1.23E–4	68889.6	–37.83
5	20	1.38E–4	60711	–31.82
6	20.6	1.64E–4	52086	–20.18
8	21.9	2E–4	42080	–0.15

Table 2. Input parameters, simulated and measured results of DRAs

Sample	Input parameters	Output parameters ( $\text{HEM}_{118}$ )	
		Simulated	Measured
92MZCST– 1 (DRA–1)	Radius (a) = 0.645 cm	$f_0 = 4.55$ GHz	$f_0 = 4.60$ GHz
	Height (h) = 0.759 cm	Return loss	Return loss
	Dielectric Constant = 21.9	bandwidth	bandwidth
	Loss tangent = 0.0002	= 100 MHz	= 315 MHz
92MZCST– 2 (DRA–2)	Radius (a) = 0.445 cm	$f_0 = 6.10$ GHz	$f_0 = 6.03$ GHz
	Height (h) = 0.715 cm	Return loss	Return loss
	Dielectric Constant = 21.9	bandwidth	bandwidth
	Loss tangent = 0.0002	= 150 MHz	= 357 MHz

### 3.2 Studies of 92MZCST DRA

The DRAs are placed above a conducting ground plane which made of copper (dimensions are 10 cm, 10 cm, 0.2 cm), and excited by a 50  $\Omega$  coaxial probes of same diameter (=0.6 mm) but different lengths (= 6.5 mm, 6 mm measured from the upper surface of ground plane) which have been optimized to provide minimum return loss at the corresponding resonant frequencies. The input and output parameters of DRAs are given in Table 2. The coaxial probe goes through the ground plane and is connected to a subminiature version A (SMA) connector. Measurement of return loss vs. frequency of both DRAs with coaxial probe feeds were carried out using Agilent PNA series Vector Network Analyzer (E8364 B). The measured variations of return loss vs. frequency for the two DRAs are shown in Fig. 3. The frequency at which return loss of a DRA, becomes minimum is called resonant frequency of the structure. The measured values of the resonant frequency and -10 dB return loss bandwidth extracted from Fig. 3 are given in Table 2 along with their theoretical values. From the measured results the resonant frequency of DRA-1 and DRA-2 are achieved at 4.60 GHz and 6.03 GHz respectively. It can be seen from Table 2 that measured resonant frequencies for the two resonators are nearly in agreement with the respective theoretical one. Deviations are observed in the measured and theoretical values of return loss bandwidth for the two DRAs. The deviations in the results may be due to the finite size of ground plane used in measurements and the edge diffraction effects.

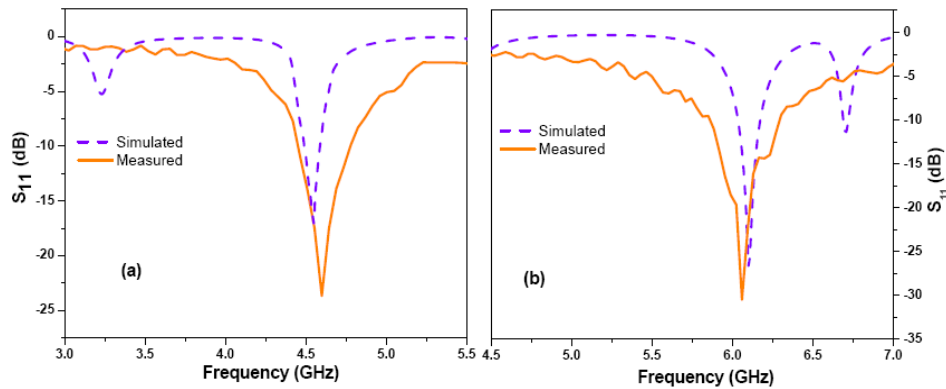


Fig. 3. Simulated and measured return loss of (a) DRA-1 and (b) DRA-2

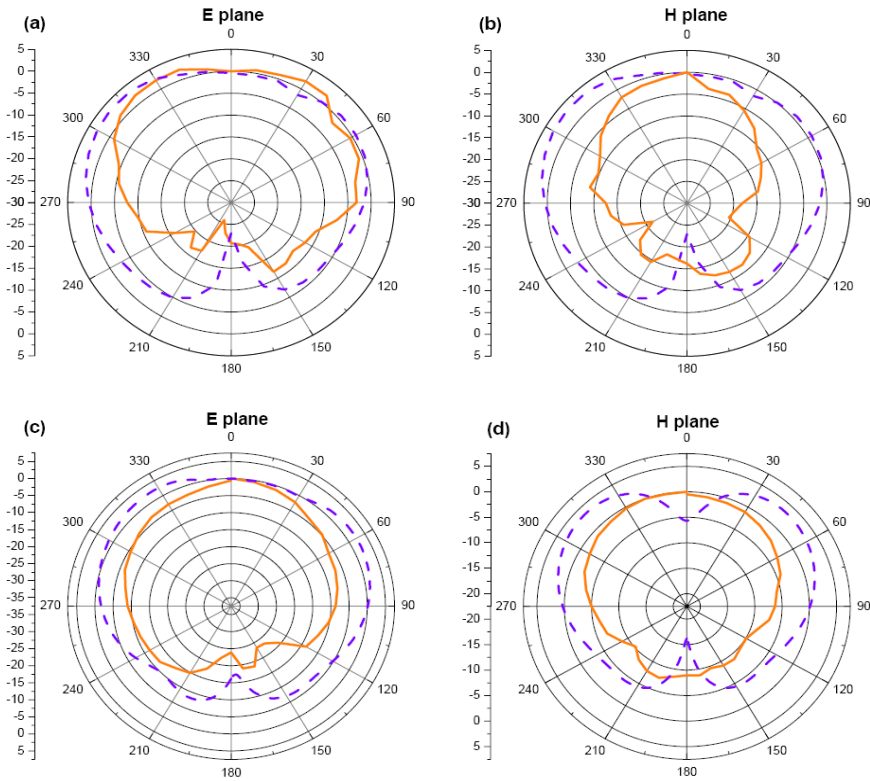


Figure 4. Simulated and measured far field radiation patterns for (a-b) DRA-1 and (c-d) DRA-2

The far field radiation patterns of both DRAs for  $\phi = 0^\circ$  (E-plane) and  $\phi = 90^\circ$  (H-plane) have been measured at the respective resonant frequencies of the antenna. It is evident from the figure that the designed antennas exhibit almost omni directional characteristic. The normalized far field radiation patterns of the DRA are shown in Fig. 4. Hence the expected resonant frequency can be obtained by choosing the permittivity and size of the antenna. The resonator frequency can be decreased or increased by choosing the materials with different permittivity and suitable size. This means such kinds of DRAs can be suitable candidates for the practical applications in the communication field.

#### 4. Conclusions

In this study, two low profile cylindrical DRAs fabricated from low loss and nearly zero  $\tan \delta$  value ceramic composites (92MZCST) are proposed. The dielectric composite samples have been prepared through the combination of



MZTO and CSTO by solid-state reaction method. From the XRD results existences of both the phases have been confirmed with an intermediate phase. The microwave dielectric properties of samples have been studied by resonator cavity method. The **0.92MZTO – 0.08CSTO** sample possesses excellent microwave dielectric properties; a dielectric constant ( $\epsilon_r$ ) of 21.9, a dielectric loss ( $\tan \delta$ ) of 0.0002, and temperature coefficient of resonant frequency ( $\tau_f$ ) of  $-0.15$  ppm/ $^{\circ}\text{C}$ . For the antenna design cylindrical disc of the sample has been placed above a ground plane, and a coaxial probe has been used for excitation which excites the  $\text{HE}_{11\delta}$  mode. The DRA-1 and DRA-2 have been presented impedance bandwidth of 315MHz and 357MHz respectively at their respective resonant frequencies. The obtained values for the E plane and H plane show a broad, almost omni-directional pattern with good radiation efficiency. From above results it is concluded that such kinds of DRAs can be suitable candidates for the practical applications.

### Acknowledgements

The Authors would like to acknowledge the members of Central Instrumentation Facility Lab, Birla Institute of Technology, Mesra for providing SEM and EDX facilities. S. Keshri gratefully acknowledges Department of Science and Technology (DST), India for financial assistance. S. S. Rajput gratefully acknowledges DST, India for providing fellowship. For the work of XRD the members of Experimental Condensed Matter Physics Division of Saha Institute of Nuclear Physics, Kolkata (India) are hereby acknowledged by the authors. The authors would like to acknowledge Dr. N. Gupta and Dr. V. R. Gupta, Department of Electronics and Communication Engineering, Birla Institute of Technology, Mesra Ranchi for providing the Antenna measurement facility.

### References

1. A. Ittipiboon and R. K. Mongia, *IEEE Transactions on Antennas and Propagation*, **45** (1997) 1348–1356.
2. R. K. Mongia and P. Bhartia, DRA– *International journal of Microwave and Millimeter wave computer –aided engineering*, **4** (1994) 230–247.
3. S. A. Long, M. W. McAllister and L. C. Shen, The resonant cylindrical dielectric cavity antenna, *IEEE Trans Antennas Propag*, **31** (1983) 406–412.
4. R. Chair and K. F. Lee, Wideband simple cylindrical dielectric resonator antennas. *IEEE Microwave Wireless Component Lett*, **15** (1997) 241–3.
5. P. V. Bijumon, Broadband cylindrical dielectric resonator antenna excited by modified microstrip line. *Electron Lett*, **41** (2005) 385–7.
6. A. A. Kishk, D. Kajfez, Broadband stacked dielectric resonator antennas. *Electron Lett*, **25** (1989) 1232–3.

7. G. Yong-Xin and L. Kwai-Man, On improving coupling between a coplanar waveguide feed and a dielectric resonator antenna. *IEEE Trans Antennas Propag* 2051; **51(8)**:20034.
8. Z. Wang, Optimisation of a broadband dielectric loaded printed antenna., *Microwave Opt Technol Lett*., **48** (2006) 1519–22.
9. P. Kingsley, G. O'Keefe, Beam steering and monopulse processing of probe fed dielectric resonator antennas., *IEE Proc Radar Sonar Navigation*, 1999; **146(3)**:121–5.
10. P. Kingsley, G. O'Keefe, Dielectric resonator antenna with mutually orthogonal feeds. US 7042416B2, 1999.
11. M. T. Sebastian, K. P. Surendran, Tailoring the microwave dielectric properties of  $\text{Ba}(\text{Mg}_{1/3}\text{Ta}_{2/3})\text{O}_3$  ceramics, *J. Eur. Ceram. Soc.*, **26** (2006) 1791–1799.
12. M. A. Sanoj, Manoj Raama Varma, Sinterability and microwave dielectric properties of  $0.95\text{MgTiO}_3$ – $0.05\text{CaTiO}_3$ –glass ceramic composites, *J. Alloys Compd.*, **477** (2009) 565–569.
13. T. S. Rao, V. R. K. Murthy, B. Viswanathan, Review of perovskite ceramics–microwave dielectric resonator materials, *Ferroelectrics*, **102** (1990) 155–160.
14. B. H. Shen, C. L. Huang, Microwave dielectric characteristics of  $(\text{Mg}_{0.95}\text{Ni}_{0.05})\text{TiO}_3$ – $\text{Ca}_{0.8}\text{Sm}_{0.4/3}\text{TiO}_3$  ceramic system, *J. Alloys Compd.*, **477** (2009) 720–725.
15. M. L. Hsieh, L. S. Chen, S. M. Wang, C. H. Sun, M. H. Weng, M. P. Houn, S. L. Fu, *Jpn., J. Appl. Phys.*, **44** (2005) 5045.
16. P. L. Wise, I. M. Reaney, W. E. Lee, Structure–microwave property relations in  $(\text{Sr}_x\text{Ca}_{1-x})_{n+1}\text{Ti}_n\text{O}_{3n+1}$ , *J. Eur. Ceram. Soc.*, **21** (2001) 1723–1726.
17. A. Belous, O. Ovchar, D. Durylin, M. Valant, M. M. Krzmancc, D. Suvorov, Microwave composite dielectrics based on magnesium titanates, *J. Eur. Ceram. Soc.*, **27** (2007) 2963–2966.
18. C. L. Huang, C. H. Shen, C. L. Pan, Calcium–doped  $\text{MgTiO}_3$ – $\text{MgTi}_2\text{O}_5$  ceramics prepared using a reaction–sintering process, *Mater. Sci. Eng. B*, **145** (2007) 91–96.
19. B. Kajfez, P. Guillon, Dielectric Resonators, in: The Artech House Microwave Library Series, 1986.
20. L. Wu, Y. C. Chen, L. J. Chen, Y. P. Chou, Y. T. Tsai, Preparation and Microwave Characterization of  $\text{Ba}_x\text{Sr}_{1-x}\text{TiO}_3$  Ceramics, *Jpn. J. Appl. Phys.* **38** (1999) 5612–5615.